Pergamon

Bioorganic & Medicinal Chemistry, Vol. 3, No. 4, pp. 429–436, 1995

0968-0896/95 $9.50 + .00

0968-0896(95)00032-1

On the Conformation of Phe78 of a Chromoprotein Antibiotic, Neocarzinostatin

Seiichi Imajo,[a] Masaji Ishiguro,[a]* Toshiyuki Tanaka,[b] Masahiro Hirama[b] and Alexei Teplyakov[c]

[a]*Suntory Institute for Biomedical Research, Shimamoto, Osaka 618, Japan*
[b]*Department of Chemistry, Faculty of Science, Tohoku University, Sendai 980-77, Japan*
[c]*EMBL, c/o DESY, Hamburg, Germany*

Abstract—A structure of neocarzinostatin, an antitumor chromoprotein antibiotic, has been built using X-ray crystallographic data and NMR data, particularly NOE data observed between the apoprotein and the chromophore. Chemical shift changes of protons of the chromophore upon binding to the apoprotein indicated that the aromatic plane of Phe52 has the conformation almost perpendicular to the C-2–C-3 triple bond of the core of the chromophore while Phe78 takes multiple conformations in solution although one of the stable conformations has been assigned for Phe78 in a crystal structure.

Introduction

Recent studies on structure analysis of a family of antitumor chromoprotein antibiotics which consist of neocarzinostatin (**1**),[1] C-1027 (**2**)[2] and kedarcidin (**3**)[3] disclosed a unique carbocyclic skeleton of the chromophores which are noncovalently bound to their macromolecular apoproteins (Fig. 1). These apoproteins stabilize their photo- and heat-labile chromophores through complex formation. Among those chromoprotein antibiotics, the three-dimensional structure of neocarzinostatin (NCS) has been most extensively analyzed by spectroscopic[4–6] and crystallographic methods.[7,8]

The structure of the non-protein chromophore of NCS in solution was elucidated with NMR spectroscopy.[9] The absolute configuration of this molecule has been determined by means of chemical synthesis of partial structures of the degradation product.[10]

NMR analysis of the three-dimensional structure of the NCS holoprotein in aqueous solution revealed the binding mode of the chromophore in the apoprotein[4] and suggested a close secondary structure of the apoprotein to that observed by X-ray crystallographic analysis.[7] Of three aromatic residues, Trp39, Phe52 and Phe78 at the chromophore-binding site, Trp39 and Phe52 formed a specific binding pocket for the naphthoate of the chromophore.[8] The Phe78 residue was located in van der Waals contact with the carbocyclic core of the chromophore, suggesting its role for the binding and stabilization of the labile unsaturated core.

In a recent crystal structure which consisted of a 1:1 mixture of the apo- and holoproteins at 1.8 Å resolution,[8] the conformation of the Phe78 side chain of the holoprotein is significantly distinct from that found in the apoprotein. Furthermore, another crystal structure at 1.5 Å resolution[7] indicates that the aromatic residue has a different conformation from those of the crystal reported by Kim *et al.*[8] Thus, we investigated conformations of the Phe78 residue in solution using NMR data observed for the chromophore at the binding site. Our modeling study using only NOE data observed between the chromophore and the apoprotein did not result in a single conformation, although the chromophore could be located at almost the same site in the binding cleft. In addition to the NOE data, we observed chemical-shift changes of several protons of the chromophore upon complex formation.[9] Hence, we examined possible conformations of aromatic residues (Phe52, Phe78, and Trp39) located at the binding cleft to determine whether those conformations explain the chemical-shift changes.

Complex structures were generated using the NOE data and the crystal structure at 1.5 Å resolution. Through this study, the Phe52 residue was found to have a single conformation. This conformation was consistent with that found in the crystals obtained at both 1.5 Å and 1.8 Å resolution, in which the aromatic face was oriented perpendicular to the C-2–C-3 triple bond of the chromophore. On the other hand, we concluded that the Phe78 residue has multiple conformations in solution since no single conformation could explain all of the chemical shift changes.

Results and Discussion

Model-building of NCS structure

The three-dimensional structure of the NCS apoprotein determined at 1.5 Å resolution[7] was available and was used as a template for the apoprotein structure in this

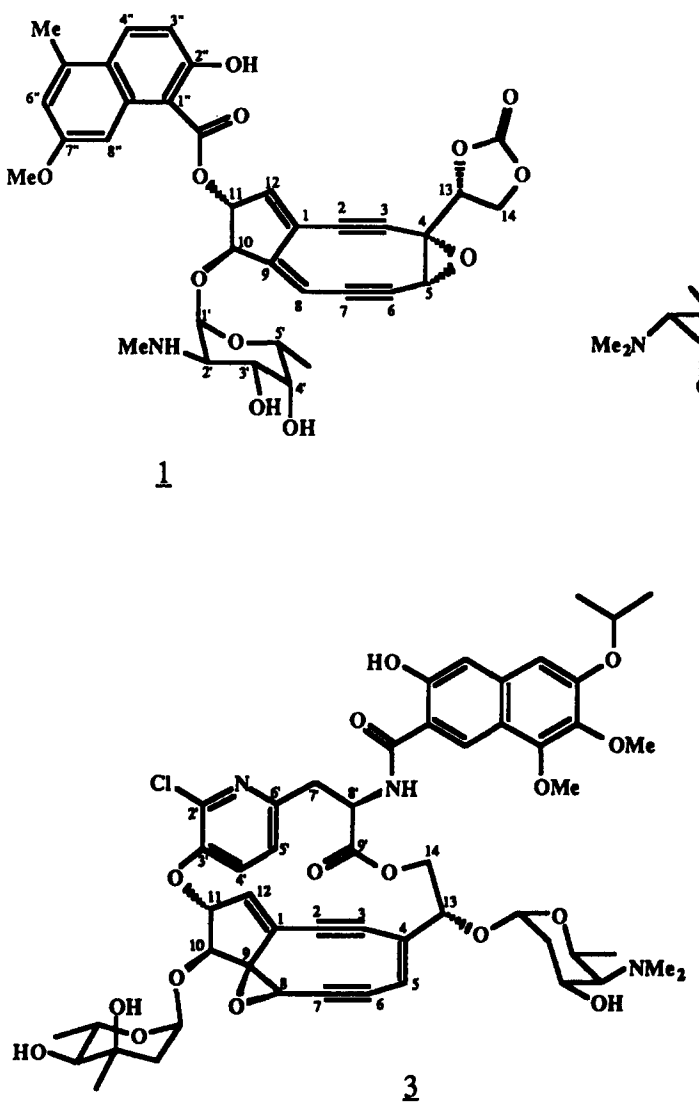

Figure 1. Structures of the enediyne antibiotic chromophores of neocarzinostatin (1), C-1027 (2), kedarcidin (3).

Figure 2. Stereoview of the 100 structures of NCS chromophore in the holoprotein generated on the basis of the constraints from NOE. These structures were superimposed in the binding cleft of the apoprotein.

Table 1. Intermolecular (A) and intramolecular (B) distance constraints used for the DGEOM calculations

A

No	Chromophore	Apoprotein		Intensity[a]	Limit[b]	No	Chromophore	Apoprotein		Intensity[a]	Limit[b]
1	H3"	Trp39	Cζ2H	m	4.0	2	H4"	Leu45	CδH3	w	7.4
3	5"-Me	Leu45	CδH3	w	8.4	4	5"-Me	Gln94	CαH	w	6.0
5	5"-Me	Gln94	CβH	s/s	4.9	6	5"-Me	Val95	CαH	w	6.0
7	5"-Me	Gly96	CαH	w/w	7.0	8	5"-Me	Gly107	CαH	w/m	7.0
9	H6"	Gln36	CαH	w	5.0	10	H6"	Val95	CαH	w	5.0
11	H6"	Gly96	NH	m	4.0	12	H6"	Gly96	CαH	w	6.0
13	7"-OMe	Asp33	CβH	m/s	6.0	14	7"-OMe	Phe52	Cδ1,2H	w	8.0
15	7"-OMe	Phe52	Cε1,2H	w	8.0	16	7"-OMe	Phe52	CζH	w	6.0
17	7"-OMe	Leu97	CαH	w	6.0	18	7"-OMe	Ser98	CβH	m	6.0
19	H8"	Ser98	CβH	m	5.0	20	H4'	Phe78	CβH	w/m	6.0
21	H4'	Phe78	arom	w	7.4	22	H5'	Leu45	CδH3	w	7.4
23	H5'	Phe78	CβH	w/s	6.0	24	H5'	Phe78	arom	w/w	7.4
25	H6'	Trp39	Cζ3H	w	6.0	26	H6'	Trp39	Cη2H	s	3.9
27	H6'	Leu45	CβH	w	7.0	28	H6'	Leu45	CδH3	m	7.4
29	2'-NMe	Phe78	arom	w/w	8.4	30	2'-NMe	Ala101	CαH	w	6.0
31	2'-NMe	Gly102	CαH	w/w	7.0	32	H5	Phe76	CβH	w/w	6.0
33	H5	Phe76	arom	w	7.4	34	H8	Leu45	CβH	w/w	6.0
35	H8	Leu45	CδH3	w/m	7.4	36	H8	Phe78	CβH	w/w	6.0
37	H8	Phe78	arom	w/w	7.4	38	H10	Leu45	CδH3	m	6.4
39	H12	Ser98	CβH	w	6.0	40	H13	Phe52	Cε1,2H	w	7.0

B

No	Chromophore		Intensity[a]	Limit[b]	No	Chromophore		Intensity[a]	Limit[b]
41	7"-OMe	H8"	s	3.9	42	7"-OMe	H12	m	4.2
43	H8"	H12	m	3.2	44	H1'	H2'	m	3.2
45	H1'	2'-NMe	m	4.2	46	H1'	H10	m	3.2
47	H1'	H11	s	2.9	48	H2'	2'-NMe	m	4.2
49	H3'	H4'	m	3.2	50	H3'	H5'	m	3.2
51	H3'	H6'	w	4.5	52	H3'	2'-NMe	w	4.5
53	H3'	H8	w	3.5	54	H4'	H5'	s	2.9
55	H4'	H6'	s	3.9	56	H5'	H6'	s	3.9
57	H5'	H8	m	3.2	58	H6'	H8	m	4.2
59	2'-NMe	H11	m	4.2					

[a]s: strong; m: medium: w: weak; [b]A: The upper-limit atomic distances derived from the observed NOEs (s ≤ 2.9, m ≤ 4.0, and w ≤ 5.0 Å). Pseudoatom correction was made for the constraints involving methylene, methyl, or aromatic ring protons. B; Intramolecular distance constraints used for the DGEOM calculations. [a]s: strong; m: medium; w: weak. [b]The upper-limit atomic distances derived from the observed NOEs (s ≤ 2.9, m ≤ 3.2, and w ≤ 3.5 Å). Pseudoatom correction was made for the constraints involving methyl protons.

model-building study. NOE data which we used here are listed in the Table 1. In the modeling, the coordinates of the apoprotein were, at first, entirely fixed during the distance geometry calculation using DGEOM[11] while those of the chromophore structure were made as flexible as possible. However, we could not generate any complex structures (holoproteins) with parameters, maxchi (Å^3) and maxdist (Å) at 0.5 (default value, see Experimental Section) respectively within one hundred trials in the distance geometry calculation. A complex structure was, however, obtained using an unusually large value of the parameters of 0.8. As expected, the chromophore obtained through this modeling had an apparently distorted structure, particularly in the carbocyclic core. Inspection of the van der Waals (vdw) contacts between the chromophore and amino acid residues at the binding site revealed that the aromatic residue Phe78 had many unreasonably short vdw contacts. Table 2 (entry 1) shows averaged distances between the chromophore and the amino acid residues in the 100 conformations generated by this calculation. Hence, the distortion of the carbocycle appeared mainly due to the wrong conformation of Phe78 of the apoprotein, one not optimal for binding of the chromophore. When the conformation of Phe78 was unlocked, we obtained 100 holoprotein structures with parameters of 0.3 or less. The generated complex structures showed no unreasonable conformational distortion in the carbocyclic core and a nice agreement with the NOE data except a slight deviation in the distance between Trp39 and C3" of the chromophore (see Table 2: entry 2, No. 23). This deviation was avoided with a minor conformational change of Trp39.

The functionality of the chromophore in all the 100 generated structures is located at similar positions in the binding site (as shown in Fig. 2). The carbocycle

Table 2. Unreasonable short distances between the chromophore and the apoprotein residues in the 100 conformations generated by the DGEOM calculation

					Entry1		Entry2	
No[a]	Chromophore	Apoprotein		Limit[b]	Ave.	SD	Ave.	SD
1	5"-Me	Gly35	O	3.05	2.98	(0.02)	3.31	(0.12)
2	Epox O	Phe52	Cε2	3.05	2.84	(0.03)	4.12	(0.21)
3	C10	Phe78	Cζ	3.30	3.23	(0.08)	4.81	(0.95)
4	C7	Phe78	Cε1	3.30	3.08	(0.02)	5.18	(0.59)
5	C8	Phe78	Cζ	3.30	3.15	(0.03)	5.10	(0.38)
6	C4'	Phe78	Cε2	3.30	3.09	(0.02)	5.77	(1.29)
7	C9	Phe78	Cε1	3.30	3.18	(0.08)	4.54	(0.97)
8	C8	Phe78	Cδ1	3.30	3.25	(0.07)	4.15	(0.65)
9	C3'	Phe78	Cε2	3.30	2.90	(0.03)	4.82	(1.03)
10	C5'	Phe78	Cε2	3.30	3.18	(0.04)	5.96	(1.06)
11	C8	Phe78	Cε1	3.30	2.55	(0.01)	4.82	(0.58)
12	C5'	Phe78	Cζ	3.30	3.17	(0.02)	6.05	(0.69)
13	C4"	Gln94	Nε2	3.20	3.04	(0.02)	3.10	(0.06)
14	5"-Me	Gly96	N	3.20	3.13	(0.03)	3.04	(0.06)
15	Ester O	Ser98	Cβ	3.05	2.99	(0.03)	4.22	(0.42)
16	C12	Ser98	Oγ	3.05	2.87	(0.01)	4.18	(0.18)
17	C11	Ser98	Oγ	3.05	2.88	(0.01)	4.38	(0.25)
18	C1'	Gly102	Cα	3.30	3.12	(0.01)	4.77	(0.31)
19	Ester Carbonyl O	Gly102	O	2.80	2.66	(0.67)	3.61	(1.41)
20	C11	Gly102	Cα	3.30	3.19	(0.02)	3.91	(0.42)
21	C6	Phe78	Cα	3.30	5.07	(0.08)	3.25	(0.08)
22	5"-Me	Gly96	N	3.20	3.13	(0.03)	3.04	(0.06)
23	H3"	Trp39	Cζ2H	4.0	4.10	(0.01)	4.04	(0.06)
24	5"-Me	Gln94	CβH	4.9	5.06	(0.02)	4.89	(0.07)
25	H4'	Phe78	CβH	6.0	6.14	(0.03)	5.32	(0.47)
26	H5'	Phe78	CβH	6.0	6.07	(0.08)	5.02	(0.36)
27	H6'	Trp39	Cη2H	3.9	4.01	(0.08)	3.45	(0.28)
28	H5	Phe76	arom	7.4	7.62	(0.01)	7.21	(0.27)

[a]Nos 1–22 : atom pairs below from vdw contacts. Nos 23–28 : atom pairs far from NOE distance constraints. [b]The lower-limit of atomic distances derived from the vdw radii used in the program DGEOM (C 1.65, N 1.55, O 1.40 Å). Ave: Average value, SD: standard deviation values.

and the naphthoate group are located at limited sites with a limited conformation. The sugar moiety also has basically one conformation while the conformation of the carbonate side chain could not be localized to a confined one with the constraint used in the distance geometry calculation. Since the NOE was observed between H-13 and an aromatic proton of Phe52, we chose the conformation in which H-13 is in proximity to Phe52. Hence, we could define an apoprotein-bound structure of the chromophore.

We observed characteristic shifts of several proton signals of the chromophore upon binding to the apoprotein in its NMR spectrum (Tables 3 and 4). H-13 showed a large downfield shift (+0.43 ppm) which can be interpreted by a deshielding effect of the proximal phenyl ring of Phe52.[12] Another large upfield shift (–1.03 ppm) of the methoxy protons is due to a close proximity to a face of the aromatic ring of Phe52 and to two main-chain amide carbonyls of Asp33 and Val34. The effect of Phe52 on the shift of the methoxy protons was calculated to be –0.49 ppm. Thus, the amide carbonyls would affect the chemical shift in a range of –0.4 to –0.5 ppm. This type of effect would also explain the upfield shift (–0.42 ppm) of the methyl group (5"-Me) of the naphthoate caused by the amide carbonyls of Gln94 and Val95 and H5 (–0.56 ppm) by the carbonyls of Leu77 and Phe78. Table 3 shows calculated chemical-shift changes of the protons of the chromophore by influences of the aromatic groups, Phe52, Trp39 and the naphthoate.

There are several conformations for the aromatic residue Phe78 in the generated structures. These can be classified into two major groups (A and B in Table 4) based on values of a dihedral angle χ_1 of the side chain of Phe78. The phenyl residue in group A locates over the carbocycle ($\chi_1 = 206° \pm 7$) while that in group B contacts at a side wall of the cleft, consisted of Gly43, Val44, and Leu45 and away from the core with a χ_1 value ($19° \pm 7$). Two typical conformations which exemplify those found in group A and B are shown in Figure 3.

The influence of the aromatic residue Phe78 on the chemical-shifts of proton signals of the chromophore in conformations of group A and B (χ_1 and χ_2 values are listed in Table 3) was estimated[12] and is shown in Table 4. These data suggest that conformations in which a face of the aromatic ring is parallel to a face of

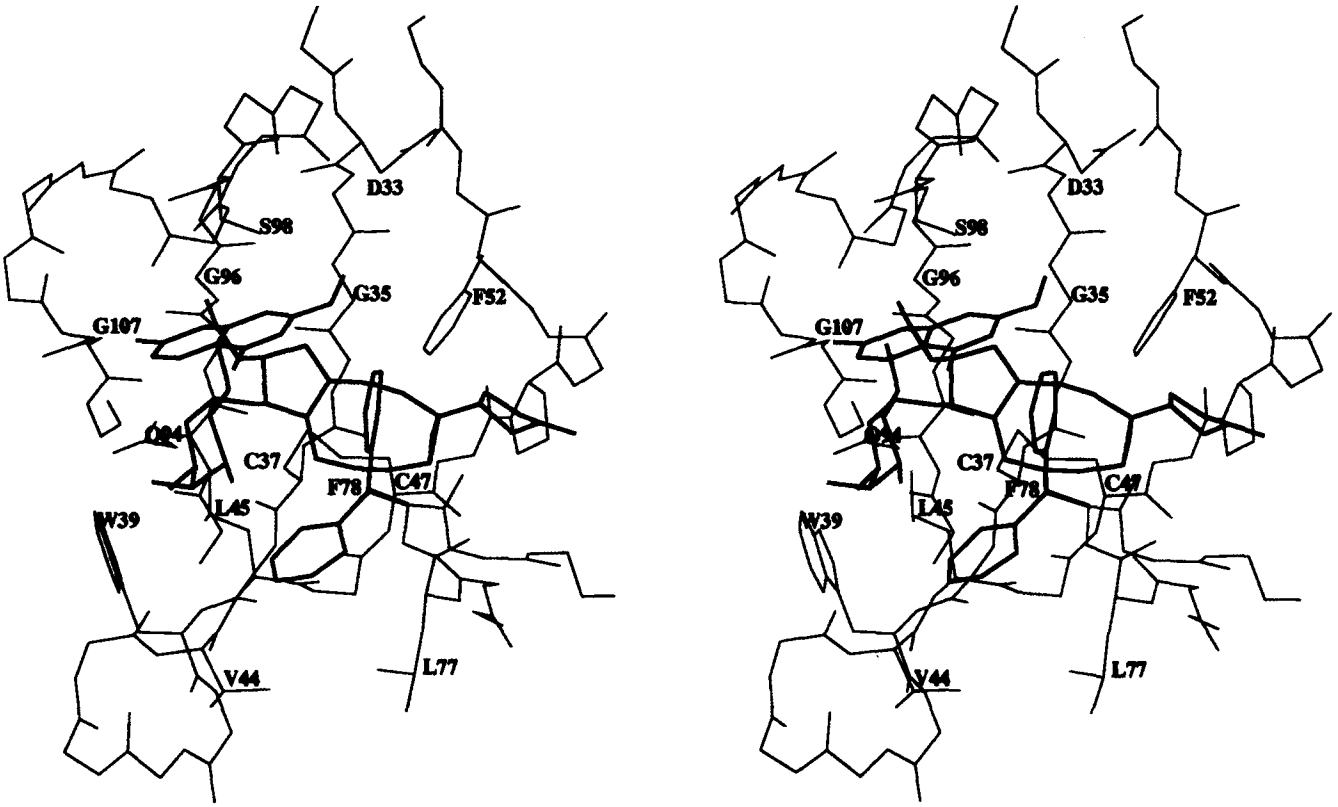

Figure 3. Stereoview of NCS chromophore (red) and the representative conformation of Phe78 in group A (conformation No. 6 sited in Table 4, green) and B (conformation No. 15, blue). Conformation No. 6 is similar to that of holoprotein in crystal and conformation No. 15 is the most stable conformer in group B. Only the side-chains located at chromophore binding cleft are shown for clarity.

the carbocycle in group A contribute to the chemical shifts of the protons at H-10 and H-11 while those of H-3' and 2'-NMe are affected by conformations in which an edge of the aromatic ring faces to the carbocycle. The influence of conformations in group B on the chemical shifts of H-4' may also be significant. However, no single conformation is able to explain all of the obseved changes of the chemical shifts. Figure 4 shows a contour map of conformational energies calculated with AMBER[13] for the residue Phe78 in a model structure of the holoprotein. Since energy barriers between the conformers in group A and B are less than 8 kcal mol^{-1}, the phenylalanine residue can equilibrate within these conformers. Thus, these results suggest that the residue Phe78 does not reside in one conformation in the solution.

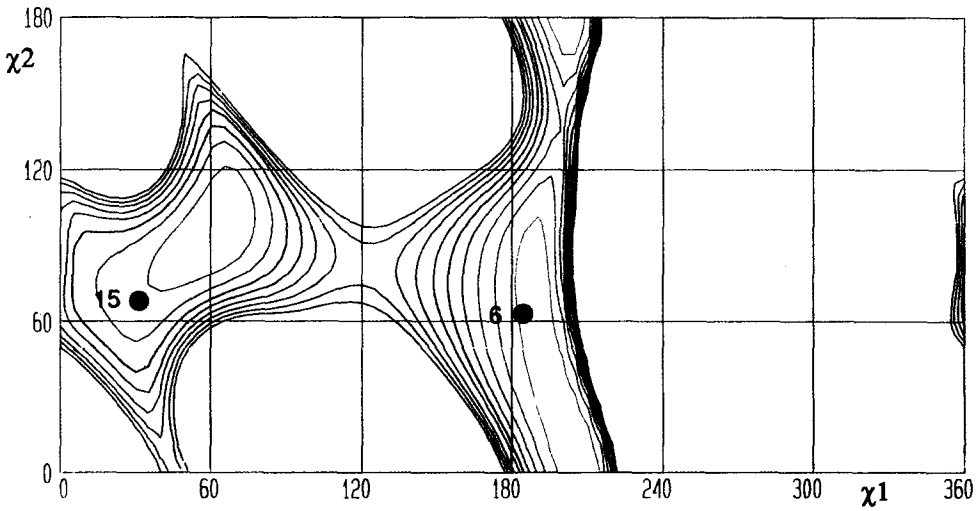

Figure 4. Contour map of the potential energy surface of Phe78 side chain (horizontal and vertical lines show the value of torsion angles χ_1 and χ_2, respectively) in NCS complex. Energy contour is shown in every 1 kcal mol^{-1} up to 10 kcal mol^{-1} from the global minimum. Filled circles indicate the position of Conformation Nos. 6 and 15 in Table 4 (see Fig. 3).

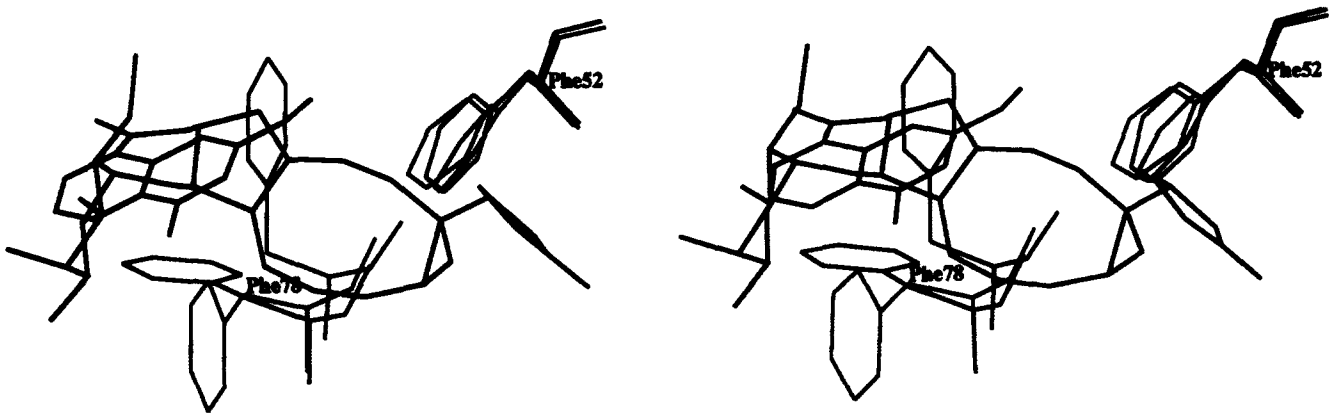

Figure 5. Conformational difference of Phe78 in holo NCS and apo NCS. Green : holoprotein,[8] blue:apoprotein,[8] red : apoprotein,[7] black:NCS chromophore.

The conformation of the residue Phe78 (χ_1 = 190° and χ_2 = 64°) in the recent crystal structure of the holoprotein[8] is close to conformation No.6 (χ_1 = 183° and χ_2 = 65°) in group A and that of Phe78 (χ_1 = 76° and χ_2 = 117°) of the apoprotein is within group B (No.15: χ_1 = 31° and χ_2 = 77°. Hence, we conclude that Phe78 in the crystal structure of the holoprotein resides in one of the stable conformers, whereas Phe78 adopts multiple conformations in solution. The aromatic–amino group interaction might explain the stability of the conformation in the crystal. However, such an interaction should not be enough to fix the phenyl residue into a sole conformation in solution. An observation that the holoprotein readily released the chromophore to form a mixture of the holoprotein and the apoprotein during crystallization[8] appears to be consistent with the observation that the original conformation of Phe78 (χ_1 = 289° and χ_2 = 164°) in the crystal structure,[7] which was used in this study, apparently differs from those reported for the holo- and apoproteins by Kim *et al.*,[8] as shown in Figure 5. This indicates that Phe78 is also able to have a different conformation in solid-phase state depending on the crystallization conditions. On the other hand, Phe52 has a single conformation which is appropriate for the interaction similar to the aromatic edge to face interaction.[15] The steric hindrance due to Phe52 and Phe78 should be important for the protection of the reactive unsaturated core in NCS rather than for the specific binding of the chromophore itself, since the naphthoate moiety is a major driving force for binding between the chromophore and the apoprotein.[16] Furthermore, it might not be irrational to assume that the tyrosine and azatyrosine unit in the chromophore of C-1027 and kedarcidin, respectively, have a similar assembly of aromatic moieties instead of Phe78 or Phe52 to stabilize the enediyne core. As we described previously,[4] the close proximity of the carbocycle to the disulfide of Cys37 and Cys47 is also likely to stabilize the chromophore in the holoprotein. Because this disulfide linkage is conserved in all apoproteins in this family, such a disulfide–core interaction would be another common factor in the family of the chromoprotein antibiotics. Thus, we conclude that among those residues mentioned above, the mobile Phe78 residue dramatically changes its conformation upon binding of the chromophore and forms a hydrophobic pocket with the disulfide bond and the aromatic moieties such as the Phe52 residue and the naphthoate group to protect the bound unsaturated core.

Experimental

NMR measurement

Solutions of NCS complex at a concentration of 5 mM in either 99.85% D_2O or 90% H_2O/10% D_2O (pH 4.0) were prepared and degassed prior to NMR measurement. NOESY[17] spectra were recorded at 30° C on a Bruker AM600 spectrometer in the pure-phase absorption mode.[18] In the case of experiments carried out in H_2O, solvent suppression was achieved by using continuous low-power irradiation during the relaxation delay (1.5 s). The carrier frequency was placed at the center of the peak of the H_2O or HOD resonance. The sweep width was 10,000 Hz. Typical sizes of data in time domains were 2,048 points for t_2 and 512 points for t_1 dimension. Prior to Fourier transformation, the data were zero-field in the t_1 dimension and multiplied by a window function (sine bell squared) in both the t_1 and t_2 dimensions. The final digital resolutions were 4.9 Hz per point in the ω_2 and 9.8 Hz per point in the ω_1 dimension.

To assess the effects of spin diffusion in the NOESY spectra of the NCS complex, a series of spectra with variable mixing times (50, 80, 100, and 200 ms) was run in D_2O and H_2O. Examination of the τ_m dependency of crosspeak volumes revealed that spin diffusion may not be a major factor for 50-ms NOESY spectra. Then, the relative peak intensities were evaluated by integrating the volume of crosspeaks in NOESY spectra with a mixing time of 50 ms. Upper bounds for intramolecular constraints in the NCS chromophore were set at 2.9, 3.2, and 3.5 Å according to the relatively strong, medium, and weak NOEs, respectively, and those for intermolecular constraints at 2.9, 4.0, and 5.0 Å. Pseudoatoms were used where no specific assignments had been made, the necessary

Table 3. Estimated shielding/deshielding effects (ppm) of the aromatic rings of Phe52, Trp39 and naphthyl moiety on the chromophore protons

Arom	H5	H8	H10	H11	H12	H13	H1'	H2'	H3'	H4'	H5'	6'Me	2'NMe	H3"	5"Me	7"OMe
Phe52	0.06	0.03	0.01	-0.01	-0.03	0.23a)	0.00	0.00	0.01	0.01	0.01	0.01	0.00	-0.01	0.00	-0.49
Trp39	-0.03	-0.07	-0.05	-0.01	-0.02	-0.02	0.00	0.02	0.00	0.02	-0.02	0.04	0.00	0.06	-0.03	-0.02
Naph1	-0.02	-0.12	-0.15	0.12	0.13	0.01	0.05	0.01	-0.02	-0.03	-0.08	-0.10	0.03	-	-	-
Naph2	-0.05	-0.12	-0.08	0.08	0.15	0.00	0.03	0.01	-0.02	-0.02	-0.04	-0.03	0.02	-	-	-
Obs	-0.56	-0.19	-0.87	-0.36	0.05	0.43	0.09	-0.03	-0.74	-0.25	-0.12	0.05	-0.39	0.25	-0.42	-1.03

[a]A calculated value for the conformation of NCS chromophore shown in Figure 3. This value changes depending on the rotation of C-4–C-13 bond.

Table 4. Conformational effect on the chemical shift change (ppm) of chromophore protons by Phe78 residue.

Group A

Conf#	χ1/χ2	H5	H8	H10	H11	H12	H13	H1'	H2'	H3'	H4'	H5'	6'Me	2'NMe	H3"	5"Me	7"OMe
1	207/-1	0.09	-0.15	-0.31	-0.31	-0.37	0.08	-0.03	0.12	0.44	0.10	-0.01	-0.01	0.17	-0.04	-0.03	-0.06
2	206/9	0.11	-0.17	-0.37	-0.38	-0.32	0.11	-0.15	0.07	0.33	0.06	-0.09	-0.04	0.13	-0.04	-0.03	-0.04
3	204/21	0.13	-0.15	-0.40	-0.41	-0.24	0.11	-0.27	-0.01	0.14	0.02	-0.17	-0.06	0.05	-0.04	-0.02	-0.02
4	197/28	0.12	-0.08	-0.32	-0.38	-0.20	0.11	-0.31	-0.06	0.02	0.01	-0.15	-0.05	-0.04	-0.04	-0.02	-0.01
5	192/38	0.11	-0.03	-0.27	-0.33	-0.12	0.09	-0.33	-0.12	-0.15	-0.02	-0.16	-0.06	-0.13	-0.03	-0.01	0.00
6	183/65	0.05	0.08	-0.11	-0.14	0.07	0.02	-0.27	-0.22	-0.45	-0.08	-0.13	-0.05	-0.24	-0.01	0.01	0.04
7	193/78	0.00	0.15	-0.04	-0.03	0.18	-0.09	-0.24	-0.24	-0.53	-0.10	-0.11	-0.04	-0.23	0.00	0.01	0.05
8	199/84	-0.03	0.21	0.01	0.03	0.23	-0.15	-0.22	-0.24	-0.55	-0.10	-0.09	-0.03	-0.23	0.01	0.02	0.05
9	188/93	-0.03	0.19	0.07	0.09	0.17	-0.13	-0.10	-0.20	-0.47	-0.08	-0.03	-0.01	-0.18	0.01	0.01	0.03
10	207/117	-0.13	0.29	0.27	0.29	0.10	-0.24	0.09	-0.11	-0.20	0.01	0.16	0.05	-0.12	0.02	0.00	-0.03
11	205/157	-0.02	-0.08	-0.03	0.05	-0.27	-0.03	0.22	0.12	0.43	0.12	0.16	0.04	0.14	-0.01	-0.03	-0.08
12	207/169	0.03	-0.24	-0.23	-0.07	-0.28	0.05	0.16	0.14	0.48	0.11	0.06	0.01	0.17	-0.03	-0.04	-0.06
Obs		-0.56	-0.19	-0.87	-0.36	0.05	0.43	0.09	-0.03	-0.74	-0.25	-0.12	0.05	-0.39	0.25	-0.42	-1.03

Group B

Conf#	χ1/χ2	H5	H8	H10	H11	H12	H13	H1'	H2'	H3'	H4'	H5'	6'Me	2'NMe	H3"	5"Me	7"OMe
13	16/42	-0.06	0.14	0.17	0.06	0.04	0.01	0.07	0.00	0.03	0.17	0.43	0.16	0.01	0.01	0.00	0.01
14	17/51	-0.07	0.35	0.18	0.06	0.05	0.01	0.04	-0.04	-0.20	-0.05	0.37	0.14	-0.01	0.02	0.00	0.01
15	31/77	-0.01	0.36	0.06	0.01	0.03	0.02	-0.04	-0.14	-0.62	-0.46	-0.01	0.02	-0.05	0.01	0.01	0.02
16	24/89	0.00	0.38	0.01	-0.01	0.03	0.03	-0.07	-0.16	-0.75	-0.74	-0.21	-0.06	-0.06	0.00	0.01	0.02
17	16/105	0.04	0.28	-0.11	-0.03	0.01	0.03	-0.10	-0.17	-0.78	-0.92	-0.54	-0.17	-0.06	-0.01	0.01	0.01
18	41/110	0.06	0.09	-0.07	-0.02	0.02	0.03	-0.07	-0.13	-0.61	-0.68	-0.30	-0.14	-0.03	-0.01	0.00	0.01
19	19/120	0.08	-0.04	-0.17	-0.04	0.00	0.03	-0.10	-0.13	-0.60	-0.85	-0.62	-0.23	-0.04	-0.02	0.00	0.01
20	13/131	0.10	-0.32	-0.25	-0.06	-0.01	0.04	-0.10	-0.09	-0.41	-0.71	-0.77	-0.28	-0.02	-0.03	-0.01	0.00
Obs		-0.56	-0.19	-0.87	-0.36	0.05	0.43	0.09	-0.03	-0.74	-0.25	-0.12	0.05	-0.39	0.25	-0.42	-1.03

Twenty out of 100 generated conformations selected in about every 10 degrees of χ_2 value are shown.

correction being added to the distance range.[19] Throughout, the lower bounds were taken as the sum of the vdw radii.

Complex structure modeling of NCS

A distance geometry program DGEOM[11] generated trial complex structures randomly and optimized the structures to minimize an error function until 100 complex structures which satisfy the distance constraints were obtained. The error function is designated as sum of the distance constraint violation and the deviations of bond length and angle from input structure. The distance constraints listed in Table 1 and those for the related atoms of Phe78 side chain (Phe78 HN–Phe78 HCβ: 5.0 Å, Phe78 HCα–Phe78HCβ: 4.0 Å, Phe78 HCα–Phe78 aromatic H: 7.4 Å and Phe78HCβ–Asp79HN: 6.0 Å) were used. Maxima of the distance violation (maxdist) and chiral error (maxchi) which is the difference of volume made by any four atoms, were restricted to be under default values (0.5 Å and 0.5 Å^3, respectively) for the calculation.

The coordinates of only 45 amino acids (Tyr32–Ser54, Gly75–Asp79, and Cys93–Ala109) which constitute the chromophore binding site were used for the distance geometry calculation. The only side-chain of Phe78 was made flexible and the other amino acid residues were kept being rigid in the calculation.

The structures obtained by this method were minimized with AMBER (steepest descent method, 300 iterations) to remove small distortions in the aromatic ring of Phe78 since a pseudoatom for the aromatic ring and a smaller vdw radii for the aromatic ring were used in the DGEOM calculation.

Energy map calculation for the conformation of the side chain of Phe78

The residues (Cys37–Val40, Gly43–Cys47, Phe52, Phe76–Thr81, and Ser98–Gly102) surrounding Phe78 and the chromophore were used for the conformational energy calculation of the Phe78 side-chain. The grid was scanned from 0 to 360° for torsion angle χ_1 and from 0 to 180° for χ_2 of the Phe78 side-chain in 5° increments. At each point of the grid, conformation energy was calculated (not minimized) using AMBER force field as implemented by MACROMODEL.[20]

References and Notes

1. Edo, K.; Mizugaki, M.; Koide, Y.; Seto, H.; Furihata, K.; Otake, N.; Ishida, N. *Tetrahedron Lett.* **1985**, *26*, 331. For apoprotein sequence: Sakata, N.; Minamitani, S.; Kanbe, T.; Hori, M.; Hamada, M.; Edo, K. *Biol. Pharm. Bull.* **1993**, *16*, 26.

2. Yoshida, K.; Minami, Y.; Azuma, R.; Saeki, M.; Otani, T. *Tetrahedron Lett.* **1993**, *34*, 2637. For apoprotein sequence: Sakata, N.; Ikeno, S.; Hori, M.; Hamada, M.; Otani, T. *Biosci. Biotech. Biochem.* **1992**, *56*, 1592.

3. Leet, J. E.; Schroeder, D. R.; Hofstead, S. J.; Golik, J.; Colson, K. L.; Huang, S.; Klohr, S. E.; Doyle, T. W.; Matson, J. A. *J. Am. Chem. Soc.* **1992**, *114*, 7946. For apoprotein sequence: Hofstead, S. J.; Matson, J. A.; Malacko, A. R.; Marquardt, H. *J. Antibiot.* **1992**, *45*, 1250.

4. Tanaka, T.; Hirama, M.; Fujita, K.; Imajo, S.; Ishiguro, M. *J. Chem. Soc., Chem. Commun.* **1993**, 1205.

5. Gao, X. J. *J. Mol. Biol.* **1992**, *225*, 125.

6. Remerowski, M. L.; Glaser, S. J.; Sieker, L. C.; Samy, T. S. A.; Drobny, G. P. *Biochemistry* **1990**, *29*, 8401.

7. Teplyakov, A.; Obmolova, G.; Wilson, K.; Kuromizu, K. *Eur. J. Biochem.* **1993**, *213*, 737.

8. Kim, K.-H.; Kwon, B.-M.; Myers, A. G.; Rees, D. C. *Science* **1993**, *262*, 1042.

9. Tanaka, T.; Hirama, M.; Imajo, S.; Ishiguro, M. manuscript in preparation.

10. Myers, A. G.; Proteau, P. J.; Handel, T. M. *J. Am. Chem. Soc.* **1988**, *110*, 7212.

11. Blaney, J. M.; Crippen, G. M.; Dearing, A.; Dixon, J. S. DGEOM, QCPE No. 590, 1990.

12. Johnson, C. E.; Bovey, F. A. *J. Chem. Phys.* **1958**, *29*, 1021.

13. Singh, U. C.; Weiner, P. K.; Caldwell, J. W.; Kollman, P. A. AMBER UCSF, version 3.0., Department of Pharmaceutical Chemistry, University of California, San Francisco, 1986.

14. Burley, S. K.; Petsko, G. A. *FEBS Lett.* **1986**, *203*, 139.

15. Burley, S. K.; Petsko, G. A. *Science* **1985**, *229*, 23.

16. Takahashi, K.; Tanaka, T.; Suzuki, T.; Hirama, M. *Tetrahedron* **1994**, *50*, 1327

17. Jeener, J.; Meier, B. H.; Bachmann, P.; Ernst, R. R. *J. Chem. Phys.* **1979**, *71*, 4546.

18. Marion, D.; Wüthrich, K. *Biochem. Biophys. Res. Commun.* **1983**, *113*, 967.

19. Wüthrich, K.; Billeter, M.; Braun, W. *J. Mol. Biol.* **1983**, *169*, 949.

20. Macromodel, V. 3.0, Department of Chemistry, Columbia University, New York, NY 10027.

(*Received in U.S.A.* 6 *June* 1994; *accepted* 19 *January* 1995)